



CHALMERS
UNIVERSITY OF TECHNOLOGY

Effect of biofuel- and lube oil-originated sulfur and phosphorus on the performance of Cu-SSZ-13 and V₂O₅-WO₃/TiO₂ SCR catalysts

Downloaded from: <https://research.chalmers.se>, 2021-08-31 12:15 UTC

Citation for the original published paper (version of record):

Dahlin, S., Englund, J., Malm, H. et al (2021)

Effect of biofuel- and lube oil-originated sulfur and phosphorus on the performance of Cu-SSZ-13 and V₂O₅-WO₃/TiO₂ SCR catalysts

Catalysis Today, 360: 326-339

<http://dx.doi.org/10.1016/j.cattod.2020.02.018>

N.B. When citing this work, cite the original published paper.



Effect of biofuel- and lube oil-originated sulfur and phosphorus on the performance of Cu-SSZ-13 and V₂O₅-WO₃/TiO₂ SCR catalysts

Sandra Dahlin^{a,*}, Johanna Englund^b, Henrik Malm^c, Matthias Feigel^d, Björn Westerberg^e, Francesco Regali^e, Magnus Skoglundh^b, Lars J. Pettersson^a

^a Department of Chemical Engineering, KTH Royal Institute of Technology, Stockholm, 10044, Sweden

^b Competence Centre for Catalysis, Chalmers University of Technology, Gothenburg, 41296, Sweden

^c Umicore Denmark ApS, DK-2800, Kgs Lyngby, Denmark

^d Department of Chemistry, TUM Technical University of Munich, 85 748, Garching, Germany

^e Scania CV AB, 151 87, Södertälje, Sweden



ARTICLE INFO

Keywords:

Cu-SSZ-13
V₂O₅-WO₃/TiO₂
NH₃-SCR
phosphorus
sulfur
biodiesel exhaust

ABSTRACT

Two different SCR catalysts, V₂O₅-WO₃/TiO₂ and Cu-SSZ-13, were exposed to biodiesel exhausts generated by a diesel burner. The effect of phosphorus and sulfur on the SCR performance of these catalysts was investigated by doping the fuel with P-, S-, or P + S-containing compounds. Elemental analyses showed that both catalysts captured phosphorus while only Cu-SSZ-13 captured sulfur. High molar P/V ratios, up to almost 3, were observed for V₂O₅-WO₃/TiO₂, while the highest P/Cu ratios observed were slightly above 1 for the Cu-SSZ-13 catalyst. Although the V₂O₅-WO₃/TiO₂ catalyst captured more P than did the Cu-SSZ-13 catalyst, a higher degree of deactivation was observed for the latter, especially at low temperatures. For both catalysts, phosphorus exposure resulted in suppression of the SCR performance over the entire temperature range. Sulfur exposure, on the other hand, resulted in deactivation of the Cu-SSZ-13 catalyst mainly at temperatures below 300–350 °C. The use of an oxidation catalyst upstream of the SCR catalyst during the exhaust-exposure protects the SCR catalyst from phosphorus poisoning by capturing phosphorus. The results in this work will improve the understanding of chemical deactivation of SCR catalysts and aid in developing durable aftertreatment systems.

1. Introduction

Selective catalytic reduction of nitrogen oxides (NO_x) by ammonia (NH₃-SCR) is today the most efficient method for abatement of NO_x from diesel exhausts in heavy-duty applications. Upcoming emission standards for heavy-duty vehicles will in addition to stringent limits for NO_x and particulate matter (PM) include limits on greenhouse gas emissions, or demands for fuel efficiency. Two strategies of reducing greenhouse gas emissions from diesel vehicles are: 1) to produce more fuel-efficient engines, and 2) to use renewable fuels, biofuels. For both cases, highly active, selective, and durable SCR catalysts are needed to meet the stringent demands for NO_x reduction. A challenge for these catalysts is deactivation related to exposure to components in the fuel or lubricant oil, such as sulfur (S) and phosphorus (P), as well as high temperatures. The effect of deactivation is particularly important at low reaction temperatures. Diesel exhausts are expected to become increasingly colder as more fuel-efficient engines are produced. In these more fuel-efficient engines, less fuel energy is wasted as heat, thus

exhausts with lower temperature are produced. The use of biofuels, such as biodiesel (fatty acid methyl esters, FAME) may introduce additional contaminants, such as phosphorus, sodium (Na), potassium (K), magnesium (Mg), calcium (Ca) and zinc (Zn), in the fuel, as compared to conventional diesel [1]. These contaminants, which originate either from the feedstock from which the biodiesel is produced, or from the production process of the biodiesel, could lead to faster deactivation of the exhaust treatment catalysts [1]. Another renewable diesel fuel is hydrotreated vegetable oil (HVO). This fuel is more similar to conventional diesel, as it consists only of paraffinic hydrocarbons, and no ester groups as does FAME. HVO meets the European diesel standard EN590, except for the density, which is lower than for conventional diesel [2].

In Europe, the concentration of S in both diesel and biodiesel (FAME) is limited to maximum 10 ppm(w) according to the fuel standards EN590 and EN14214, respectively. The European biodiesel standard (EN14214) furthermore limits the P concentration to maximum 4 ppm(w), while Na + K, and Ca + Mg must be ≤ 5 ppm(w). [1]

* Corresponding author.

E-mail address: sanj@kth.se (S. Dahlin).

<https://doi.org/10.1016/j.cattod.2020.02.018>

Received 19 October 2019; Received in revised form 18 January 2020; Accepted 19 February 2020

Available online 21 February 2020

0920-5861/ © 2020 The Author(s). Published by Elsevier B.V. This is an open access article under the CC BY-NC-ND license

(<http://creativecommons.org/licenses/by-nc-nd/4.0/>).

Using these numbers for calculating a possible total life-time exposure of S and P to catalysts in a heavy-duty diesel exhaust treatment system, Granstrand et al. [1] concluded that a substantial amount of S and P could end up in the exhaust treatment catalysts: in total around 2.4 and 0.8 kg of S and P, respectively. Furthermore, additional contributions of S and P from the lubricant oil is expected [1]. It is thus of major importance to understand how much of these contaminants that can be captured in different catalysts, and the subsequent effect on the catalytic performance.

Two different types of SCR catalysts that are used commercially in heavy-duty applications today are Cu-SSZ-13 and V_2O_5 - WO_3 /TiO₂. These catalysts display different advantages and disadvantages. For example, Cu-SSZ-13 has by far the best low-temperature performance, but may suffer from deactivation by sulfur/SO_x [3]. V_2O_5 - WO_3 /TiO₂ on the other hand, is considered robust towards sulfur, but for a good low-temperature performance, it is dependent on an upstream diesel oxidation catalyst (DOC) that can supply NO₂ to yield fast SCR conditions [4].

As there are always traces of phosphorus and sulfur in the exhaust, it is important to understand how these contaminants affect the catalytic performance of SCR catalysts. Furthermore, it is important to understand whether any observed deactivation is reversible or irreversible, and what regeneration strategies that could be used. The influence of phosphorus and sulfur on Cu-SSZ-13 SCR catalysts has been studied previously. However, there are only a few studies related to phosphorus exposure [5–8], which of most use wet impregnation to expose the catalysts for phosphorus [5,6,8]. Wet impregnation is a simple and quite exact method for introducing poisons; however, it might not reflect actual conditions in e.g. a truck. The combined conclusions from these studies are not totally clear. However, they suggest that the deactivation of Cu-SSZ-13 by phosphorus could be severe but seem to depend on the concentration of phosphorus on the catalyst, or more importantly, the molar P/Cu ratio. Low P/Cu ratios appear to result in a suppression of NH₃ and NO oxidation reactions while the standard SCR reaction is unaffected, or even slightly promoted at high temperatures [6–8]. Higher P/Cu ratios, on the other hand, could be detrimental [5,7,8]. Furthermore, there are indications that vapor-phase deposition of phosphorus [7] results in a more severe deactivation than do wet impregnation methods [6]. Moreover, sulfur poisoning of P-exposed a Cu-SSZ-13 catalyst by SO₂ has been observed to be accelerated, due to a lower amount of active Cu²⁺ in the P-poisoned catalysts [8]. In addition to these laboratory studies, Dahlin et al. [9] observed deactivation of a Cu-SSZ-13 catalyst that had been exposed to conventional diesel exhausts in an engine-cell. This catalyst had captured both sulfur and phosphorus during the engine-cell test, and only a small fraction of the deactivation was found to be due to reversible sulfur deactivation.

The effect of P on V_2O_5 - WO_3 /TiO₂ has been studied more extensively [10–16], since this type of SCR catalyst has been used for longer times, both in stationary and mobile applications. In general, it appears as the V_2O_5 - WO_3 /TiO₂ catalyst is rather tolerant towards

phosphorus; only exposure for high P concentrations (around 2 wt% and above) results in severe deactivation of the catalyst [1]. However, most of these studies used wet impregnation for the phosphorus exposure, and importantly, some studies showed that aerosol aging resulted in more severe deactivation than wet impregnation for the same phosphorus loading [11,14]. Moreover, a considerable degree of deactivation has been observed for a truck operated on FAME for around 10,000 h; high concentrations of contaminants, such as phosphorus, were found on this catalyst [17,18].

In summary, it appears as it is of major importance to elucidate the potential of both types of SCR catalyst to capture phosphorus during exposure to diesel exhausts, as well as understanding the corresponding effect on the catalytic performance.

Exposure to sulfur oxides (SO_x, x = 2 or 3) is known to result in severe deactivation of the low-temperature performance of Cu-SSZ-13 [8,9,19–26], while V_2O_5 - WO_3 /TiO₂ catalysts are sulfur tolerant and could even be slightly promoted by SO₂ exposure [4]. However, at high SO₂ concentrations in the exhaust, these catalysts could also suffer from deactivation by fouling of ammonium sulphate or bisulphate [1,4]. Most of the sulfur in the exhaust is in the form of SO₂. However, in the presence of an oxidation catalyst in front of the SCR catalyst, a significant amount of the SO₂ can be oxidized to SO₃ and/or H₂SO₄. [27] For Cu-zeolite SCR catalysts, exposure to SO₃ could cause a more severe deactivation than SO₂ [20,27,28].

In this contribution, we perform an aging study that is closer to real operating conditions than the laboratory studies mentioned above. Two different SCR catalysts, V_2O_5 - WO_3 /TiO₂ and Cu-SSZ-13, are exposed to biodiesel exhausts generated by a diesel burner. The effect of phosphorus and sulfur on the SCR performance of these catalysts is investigated by doping the fuel with P- and/or S-containing compounds. Both P and S are important for petroleum-derived diesel fuel, HVO, and biodiesel, while, the importance of P increases when biodiesel (i.e. FAME) is used. Elemental analyses are performed to determine how much of each contaminant that is captured in the different SCR catalysts, and this is furthermore correlated to the performance loss. The results of this work will improve the understanding of chemical deactivation of SCR catalysts and aid in developing durable aftertreatment systems.

2. Experimental

This work consists of performance tests and elemental analyses of fresh and aged SCR catalysts, according to the experimental procedure shown in Fig. 1. First, the performance of the fresh catalyst samples was tested; thereafter these catalysts were exposed to exhausts from combustion of pure, P-, S-, or P + S-doped FAME using a diesel-burner aging rig. For part of the aged catalyst samples, a repeated performance test was executed. Elemental analyses of all aged samples were performed, after the SCR performance had been tested, to quantify the amounts of contaminants captured in these catalysts. Additional

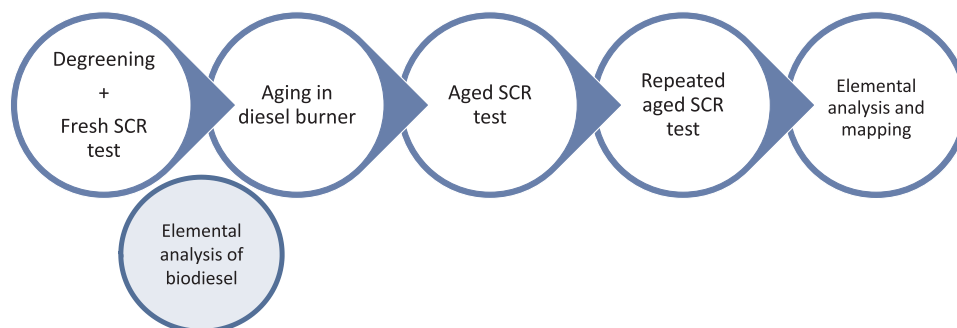


Fig. 1. Overview of the experimental procedure including fresh and aged SCR performance tests, aging and elemental analysis of biodiesel and aged catalysts. The repeated aged SCR test was performed for parts of the samples.

Table 1

Details about the SCR catalysts (Cu-SSZ-13 and $V_2O_5-WO_3/TiO_2$) used in this study. Small cores ($\varnothing = 21$ mm, $L = 30$ mm) were drilled out from full-size catalysts for both SCR catalysts and the DOC.

	Cu-SSZ-13	Commercial $V_2O_5-WO_3/TiO_2$
Composition	In washcoat: 3 wt% Cu; Si/Al = 7	In the entire catalyst: 2.3 wt% V_2O_5 , 8 wt% WO_3
Cell geometry/cell density	400 cpsi, washcoated on cordierite	260 cpsi, $V_2O_5-WO_3$ -impregnated fiberglass-reinforced TiO_2 in a corrugated shape
Washcoat loading	143 g/dm ³	-

elemental analysis of relevant contaminants in the fuel used for the different aging experiments was performed. Each of the steps in Fig. 1 is described in more detail in subsequent sections.

2.1. Catalyst materials

Two different SCR catalysts were investigated in this study: a Cu-SSZ-13 and a commercial $V_2O_5-WO_3/TiO_2$ catalyst (see Table 1). In addition to these SCR catalysts, a Pt-Pd/ Al_2O_3 DOC (Pt:Pd = 2:1, 20 g PGM/ft³) was included in the aging experiments. This DOC was positioned upstream of parts of the SCR catalysts during the aging in the diesel burner, to investigate effects of different aging configurations.

2.2. SCR performance tests

The SCR performance of fresh and aged catalysts was evaluated in a bench flow reactor, which has been described previously [9,29]. The test protocol used for evaluation of fresh and aged catalysts include the following steps: 1) NO oxidation, 2) NH_3 saturation/storage, 3) standard SCR reaction at three different O_2 concentrations, and 4) reaction of $NO + O_2$ with pre-adsorbed NH_3 . All these steps are performed at six different temperatures between 200 and 500 °C. This protocol has been used previously by Bergman et al. [29].

For most of the fresh catalyst samples, the SCR performance was evaluated from high to low temperature. This order was decided to decrease the time needed for the test, as the test was started directly after the degreening at 500 °C. For aged samples, on the other hand, the performance was evaluated from low to high temperature. This was due to that any contingent removal of sulfur should occur as late as possible in the performance test, such that any effect of sulfur desorption would be significant only in the final parts of the test.

2.3. Aging in the diesel burner rig

2.3.1. Aging rig setup

The aging of the catalyst samples was performed in an aging rig (see Fig. 2) using a diesel burner fueled with either pure, P-, S-, or P + S-doped biodiesel. This rig consists of a fuel feed (fed from a tank outside the lab, around 40 m of $1/4$ " tubings), an air feed (supplied by an air

blower), a diesel burner (Sterling 25), a heat exchanger, a cooling air blower, and a vertical multichannel reactor with nine parallel channels. Furthermore, a static mixer is positioned downstream of the burner before the reactor to ensure well-mixed gases. A lambda-sensor measures the oxygen concentration 120 mm before the reactor, and the total pressure is measured 20 mm before the reactor. The temperature is measured at several different positions in the rig including at the following points: at the burner, 120, and 20 mm before the inlet of the reactor, and 190 mm after the reactor. Additionally, an external thermocouple was connected to the inlet of one of the channels in the reactor (channel 2, see Fig. 2). The aging temperature was set to be approximately 450 °C, which currently was the lowest possible temperature for achieving a stable operation of the diesel burner. The average actual temperature during the aging varied somewhat for the different aging experiments (see Table 3), but it was always close to 450 °C. During the aging, a temperature difference of around 55 °C was measured between the thermocouple positioned in the inlet of the reactor and the thermocouple positioned 190 mm after the reactor.

The reactor consists of a stainless-steel sample holder with nine parallel channels (see Fig. 2b, c). Thus, the total exhaust flow is split into nine sub-flows during the aging experiment. In each experiment, SCR catalyst cores were positioned in four of the channels (channel 2, 4, 6, and 8); in two of these, DOC cores were positioned upstream of the other two SCR catalysts, while dummies were positioned upstream of the other two SCR catalysts. The remaining five channels were filled with two dummies positioned after each other in the same way as in the channels with the DOC/dummy-SCR catalyst samples. This was done in order to minimize flow differences through the different channels. By dummy, we mean a cordierite core of the same size as the SCR catalysts and the DOC, but without any washcoat.

2.3.2. Catalyst configuration during the aging

In each aging experiment, two $V_2O_5-WO_3/TiO_2$ and two Cu-SSZ-13 SCR catalyst cores were included. As mentioned previously, one of each type of these SCR catalyst samples had an upstream DOC core during the aging, while the other had an upstream dummy, as indicated in Fig. 2b. The effect of having a DOC in front is two-fold: one is the ability of the DOC to oxidize SO_2 in the exhaust into SO_3 , and the other is that the DOC core could act as a trap and capture poisons. Thus, the SCR

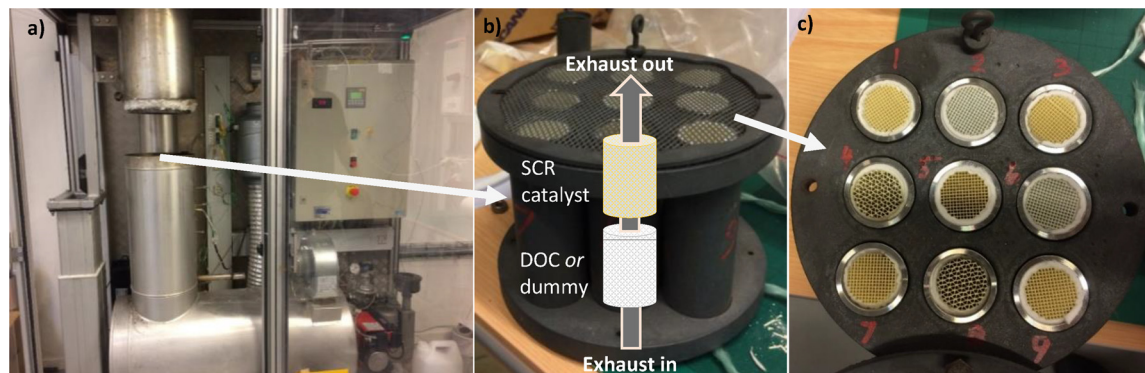


Fig. 2. The diesel burner aging rig (a) and sample holder (b and c). For each aging, the sample holder was loaded with 4 SCR catalyst cores, 2 DOC cores (in front of two of the SCR catalysts) and the remaining channels (1, 3, 5, 7, 9) were filled with dummies.

Table 2

Experimental conditions during the degreening and the SCR performance test. All temperature ramps were performed in N₂, while H₂O was present in all other steps. O₂ was present in all steps except the NH₃ storage step.

Experimental step	Test conditions
Degreening of fresh catalysts	1h, 500 °C, 10% O ₂ , 5% H ₂ O, GHSV 120,000 h ⁻¹
SCR performance test of fresh and aged catalysts	The following steps at each temperature (200, 250, 300, 350, 400, 500 °C, 5% H ₂ O all the time except for during temperature ramps. Balance N ₂ , GHSV 120,000 h ⁻¹) 1 NO (500 ppm, 1000 ppm) + O ₂ (2, 5, 10%) 2 NH ₃ saturation (1200 ppm, 1000 ppm, 500 ppm) 3 Standard SCR reaction with: a) 2% O ₂ , 1000 ppm NO and NH ₃ b) 5% O ₂ , 1000 ppm NO and NH ₃ c) 10% O ₂ , 1000 ppm NO and NH ₃ d) 5% O ₂ , 500 ppm NO and NH ₃ 4 Reaction with pre-adsorbed NH ₃ : 1000 ppm NO, 10% O ₂

Table 3

Details regarding the aging experiments with pure and doped biodiesel. The fuel was a FAME from Preem, fulfilling the European standard for biodiesel (EN14214).

	Pure FAME	P-doped	S-doped	P + S-doped
Dopant	-	TPP	DPDS	TPP + DPDS
P conc. (ppm(w))	< 0.3	93	0.5	11
S conc. (ppm(w))	2.5	2.5	130	11
Total molar exposure of P ^a : P/Cu ; P/V	< 0.3; < 0.2	104 ; 54	0.6; 0.3	12.5 ; 6.7
Total molar exposure of S ^a : S/Cu ; S/V	2; 1	2; 1	100 ; 56	9.5 ; 5.1
Average inlet temperature (°C)	440	440	455	442
Approx. amount of fuel consumed (dm ³)	185	190	190	195
Total aging time (h)	157	149	140	178

^a Total molar exposure of added S and P per copper and vanadium during the whole aging time, assuming that the flow through all nine channels in the multichannel reactor are similar, and that all V and Cu cores contain the exactly same amount of V and Cu, respectively, and furthermore assuming no contamination from previous aging experiment.

catalyst would be exposed to less contaminants. The aging temperature stated in Table 2, is the temperature just before the DOC core in channel 2.

2.3.3. Determination of dopant concentrations: life-time exposure of P and S

Four different aging experiments were performed in this study: one with pure biodiesel (FAME) serving as a baseline aging, one with P-doped biodiesel, one with S-doped biodiesel, and finally, one with both P and S doped in the fuel. In each aging experiment, approximately one barrel (200 dm³) of biodiesel was used (more details provided in Table 3). The single aging experiments with only phosphorus or sulfur were targeted to expose the catalysts to one full life-time exposure of P and S from the fuel. This life-time was defined as defined as 700,000 km, according to the Euro VI standard, and the fuel considered is a biodiesel fulfilling the EN14214 standard. In this standard, the maximum allowed concentration of phosphorus is 4 ppm, while the maximum sulfur concentration is 10 ppm(w), i.e. the same sulfur-limit as in petroleum-derived diesel fuel. However, the sulfur content in biodiesel is often lower than in the petroleum-derived fuel [1]. Therefore, when calculating the amount of phosphorus and sulfur needed for these aging experiments, we assumed the P and S concentration in a standard biodiesel to be 4 and 5 ppm(w), respectively. Additional assumptions for the calculation included a fuel consumption of 30 kg/100 km and a catalyst weight of around 5 kg. Based on these assumptions, a full life-time exposure of P and S was calculated to be 168 g P and 420 g S per kg catalyst. Worth noting though, is that commercial biodiesel often contains less than 4 ppm P and 5 ppm S, but on the other

hand, lube-oil contributes with additional amounts of S and P in real applications.

For the final aging experiment, with both P and S added to the fuel, it was decided to lower the dopant concentrations to approximately 1/10th of the trials with only P- or S-doped fuel. That is, roughly 1/10th of a life-time exposure was. This was decided as we noted a severe deactivation for both types of SCR catalysts after the exposure to the P-doped biodiesel. Furthermore, it was considered interesting to investigate the effect of the contaminants at concentrations closer to those in real applications.

In all aging experiments, the total amount of contaminants that the catalysts were exposed to was significantly higher than the amount of copper/vanadium in the catalyst. Thus, even if there would have been a slightly different flow in the different channels of the reactor due to small differences in flow restrictions, the P and S-exposure should have been more than enough to saturate all possible Cu and V sites in the catalyst samples.

2.3.4. Biodiesel and preparation of doped biodiesel

The FAME fuel used in this work was a rape methyl ester from Preem, which fulfilled the EN14214 standard according to the quality certificate from the manufacturer. This means that the concentration of Na + K and Mg + Ca is below 5 ppm(w), P below 4 ppm(w), and S below 10 ppm(w). Two different batches were used for the aging experiments; the first batch was used for aging 1-3, while a new batch was used for the 4th aging experiment. The actual numbers from the quality certificate plus our own elemental analyses of the biodiesel are included in the Supplementary Information, Table S1. In addition to the elements found in the biodiesel standard, the concentration of zinc was also measured, as Zn can be a contaminant in biodiesel when a heterogeneous catalyst is used for the biodiesel production. In both batches of FAME, the Zn concentration was around 1 ppm(w).

The dopants used for phosphorus and sulfur were triphenyl phosphate (TPP, containing 9.5 wt% P) and dipropyl disulfide (DPDS, containing 42.7 wt% S), respectively. The measured concentrations of S and P in pure (batch 1) and doped (batch 1 and 2) FAME for all aging experiments are shown in Table 3.

The TPP was in form of solid granulates. These granulates were dissolved in a part of the biodiesel from the barrel subsequently used for the aging. For this dissolution, the TPP-biodiesel blend was mixed with a magnetic stirrer over-night prior to adding the mixture to the biodiesel barrel. The DPDS was in form of a liquid that was easily dissolved in the biodiesel, and thus was added in pure form to the barrel. The barrel with added TPP or DPDS was then shaken to mix the components before the start of the aging.

2.4. Elemental analysis and mapping

Elemental analyses were performed for all aged and tested Cu-SSZ-13 and V₂O₅-WO₃/TiO₂ samples to determine the concentrations of any

captured contaminants. The following elements were analyzed in all catalysts: P, S, Ca, Mg, Na, and Zn. Furthermore, V, W, and Ti were analyzed for the V_2O_5 - WO_3 /TiO₂ catalysts and Cu, Al, and Si for the Cu-SSZ-13 catalysts. Fresh samples were analyzed as well, and additionally one of the dummies that had been positioned in front of an SCR catalyst during all aging experiments. A Leco sulfur analyzer was used for analyzing sulfur in all samples. ICP-OES was used for analyzing Zn in the V_2O_5 - WO_3 /TiO₂ samples, and a Rigaku energy dispersive X-ray fluorescence (XRF) analyzer was used for all other elements (samples prepared as a fusion bead). All catalyst cores were divided into an inlet part and an outlet part. These parts were then analyzed separately to determine if any axial concentration gradients were present within the samples. Around 1.2 g of sample was needed for analyses of Cu-SSZ-13 samples, and 1.5 g for the V_2O_5 - WO_3 /TiO₂ samples.

SEM images were obtained using a Carl Zeiss FE-SEM (Sigma VP) electron microscope with a variable pressure secondary electron detector. Elemental mapping was performed by energy-dispersive X-ray spectroscopy (EDX) using an X-Max 50 detector from Oxford Instruments. To get a flat, smooth surface, cross-section of samples were casted in epoxy. These were then analyzed in low-vacuum (40 Pa) to minimize charging effects and with an acceleration voltage of 20 kV. At least 1,000,000 counts were used for the mapping. In addition, SEM-EDX analyses were also performed on the washcoat from the wall of some of the Cu-SSZ-13 samples (these were not casted in epoxy). In this case, high-vacuum could be used.

Samples from both batches of biodiesel, pure as well as P, S-, and P + S-doped, were analyzed by ICP-OES.

3. Results and discussion

3.1. Performance of fresh Cu-SSZ-13 and V_2O_5 - WO_3 /TiO₂

After degreening, the SCR performance of all fresh Cu-SSZ-13 and V_2O_5 - WO_3 /TiO₂ catalyst cores was measured prior to the aging experiments with the diesel burner. This was done in order to be sure of that any aging effect observed was truly caused by the aging experiment, and not due to an initially lower performance of any of the

catalyst cores. In this test, the performance during the standard SCR reaction was evaluated at three different oxygen concentrations (Fig. 3, black curve: 10% O₂; grey curve: 5% O₂; blue curve: 2% O₂). Both types of catalysts, displays some differences in NO conversion, NH₃ conversion, and N₂O production as result of these different oxygen concentrations. However, this oxygen dependence differs between the two different catalysts. For the Cu-SSZ-13, a clear dependence of the oxygen concentration is observed at the lowest temperature evaluated (200 °C), where the NO and NH₃ conversions increase with increasing O₂ concentration. Furthermore, the effect of the oxygen content is most pronounced for the lowest oxygen concentration (2% O₂). For this concentration, a seagull-shape can be observed for the NO conversion profile, i.e. first an increase in NO conversion with temperature at low temperatures, followed by a decrease in conversion at intermediate temperatures (here seen at 350 °C), and finally an increase again at higher temperatures. This effect is often seen for Cu-SSZ-13 at demanding conditions, such as low Cu content, high space velocity, and low oxygen concentration [30]. As opposed to at low temperature, the NO conversion at 500 °C is slightly higher for the lowest oxygen concentration. The small drop in NO conversion observed at this temperature, is lowest when only 2% O₂ is present. Contrary to the NO conversion at 500 °C, the NH₃ conversion does not decrease. This indicates that some NH₃ oxidation by oxygen occurs at this temperature [31]. Furthermore, this oxidation appears to be favored by a higher oxygen concentration. As only a minor amount of N₂O is produced at this temperature, the main product of this NH₃ oxidation is likely N₂, making less NH₃ available for reaction with NO. For the V_2O_5 - WO_3 /TiO₂ catalyst, the NO and NH₃ conversions (Fig. 3, lower left and middle panel, respectively) are slightly higher when more oxygen is present; this applies over the entire temperature range. Further on, the NO conversion decreases significantly at high temperature (500 °C), while the NH₃ conversion remains high. Similar as for the Cu-SSZ-13, this is due to an unwanted NH₃ oxidation by O₂; however, the magnitude of this parasitic oxidation is higher than for the Cu-SSZ-13 catalyst. Moreover, the product distribution differs, as can be seen by the high formation of N₂O for the V_2O_5 - WO_3 /TiO₂ catalyst at this temperature (Fig. 3, lower panel to the right), which contrasts to the Cu-SSZ-13

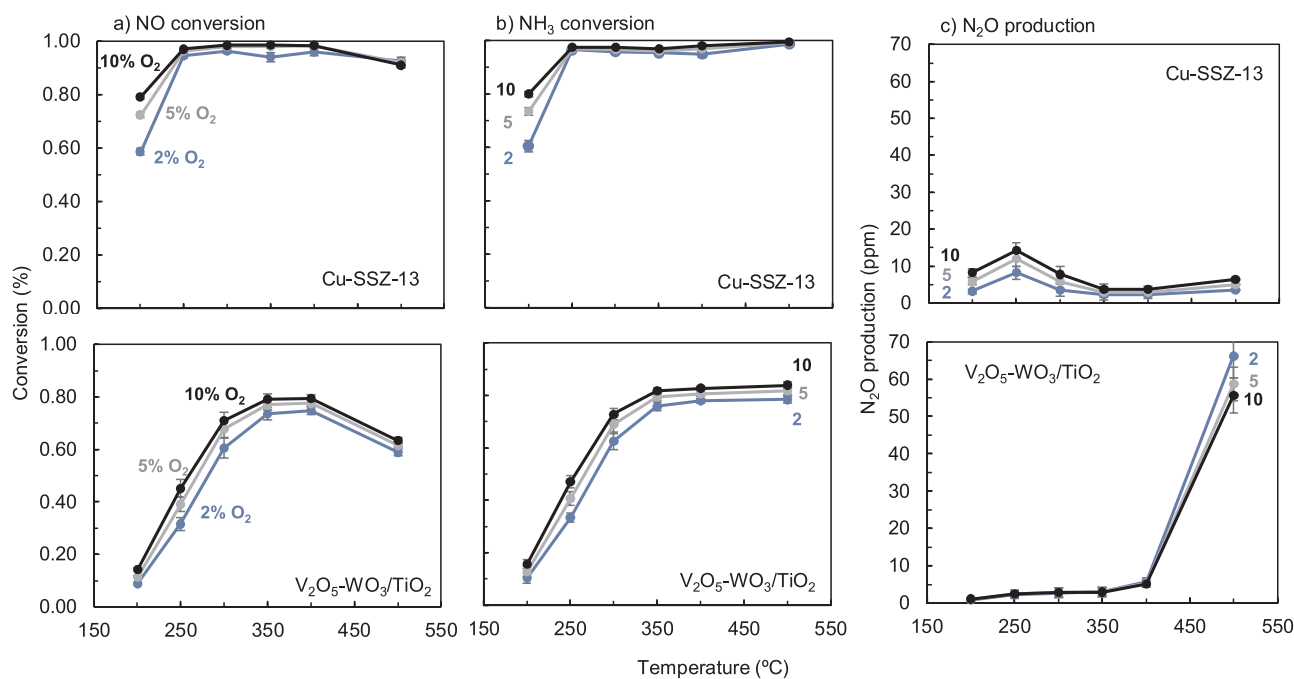


Fig. 3. Fresh SCR performance of Cu-SSZ-13 (top panel) and V_2O_5 - WO_3 /TiO₂ (lower panel). NO conversion (a), NH₃ conversion (b), N₂O production (c) at different O₂ concentrations; 2% (blue); 5% (gray); 10% (black). Test conditions: 1000 ppm NO and NH₃, 5% H₂O, GHSV 120,000 h⁻¹. Error bars show +/- 1 standard deviation.

catalyst that has low formation of N_2O at high temperature. Ammonia can, except from acting as a reductant in the SCR reactions, be oxidized into NO , N_2O and N_2 . In all these cases, the conversion of NO becomes reduced while the NH_3 conversion remains high.

N_2O is a strong greenhouse gas; consequently, the production of N_2O over the SCR catalyst needs to be low. The mechanism of N_2O formation during standard SCR conditions depends on the temperature: formation of N_2O at low temperatures (below around $300^\circ C$) is generally considered to occur through thermal decomposition of ammonium nitrates formed on the surface of the catalyst [32,33]. This N_2O production is favored if NO_2 is present in the feed [9,31,34]. The high-temperature N_2O production, on the other hand, occurs by unselective ammonia oxidation [31]. The N_2O production profiles of the two different types of SCR catalysts differ considerably. The Cu-SSZ-13 catalyst displays a maximum in N_2O production at a rather low temperature, around 14 ppm at $250^\circ C$ (the numbers in Fig. 3 are without subtracting the N_2O produced in an empty reactor, see Supplementary information, Fig. S1). In contrast, insignificant N_2O formation is observed below $400^\circ C$ for the $V_2O_5-WO_3/TiO_2$ catalyst. However, at $500^\circ C$, the N_2O formation is substantial for this catalyst; almost 70 ppm is produced under the test conditions applied in this study. Another difference is the effect of oxygen concentration on the N_2O formation. For the Cu-SSZ-13 samples, less N_2O is formed for a lower oxygen concentration. This applies over the entire temperature range, although most pronounced at temperatures below $350^\circ C$ where the formation of N_2O is highest. As opposed to this, the $V_2O_5-WO_3/TiO_2$ catalyst yields the highest N_2O production for the lowest oxygen concentration, easiest observed at $500^\circ C$ where the highest amount of N_2O is produced for this catalyst.

Comparing Cu-SSZ-13 and $V_2O_5-WO_3/TiO_2$ catalysts at the same test conditions, with the same catalyst volumes, although different cell densities, the Cu-SSZ-13 catalyst clearly has a better SCR performance than the $V_2O_5-WO_3/TiO_2$, especially in terms of low-temperature NO conversion and selectivity at high temperatures. Furthermore, the Cu-SSZ-13 samples reach almost 100% NO conversion, while $V_2O_5-WO_3/TiO_2$ samples never reach a conversion of more than around 80% during these tests. However, this could in part be due to the lower cell density of the $V_2O_5-WO_3/TiO_2$ catalyst used in this study. External mass transfer limits this catalyst to reach higher conversions [4]. Also note that for the $V_2O_5-WO_3/TiO_2$ catalysts, the space velocity used in this work ($GHSV\ 120,000\ h^{-1}$) is challenging; for this catalyst, more commonly applied $GHSV$ s applied in heavy-duty applications are between 20,000 and $70,000\ h^{-1}$ [4]. Furthermore, the fast SCR condition is often applied by having a DOC upstream of the $V_2O_5-WO_3/TiO_2$ SCR catalyst [4]. This considerably improves the low-temperature SCR performance (see Supplementary information, Fig. S2).

3.2. Performance of Cu-SSZ-13 and $V_2O_5-WO_3/TiO_2$ exposed to pure, P- and S-doped biodiesel exhaust

After the SCR performance had been tested, the fresh Cu-SSZ-13 and $V_2O_5-WO_3/TiO_2$ cores were exposed to exhausts of either pure, P-doped, S-doped, or P + S-doped biodiesel. In each aging, almost $200\ dm^3$ of fuel was used, during approximately 160 h, at a temperature of around $450^\circ C$. During this exposure, two different configurations were used: the SCR catalyst cores were positioned downstream of either a DOC core or a dummy. All the aged catalyst samples were then subjected to the same test protocol as the fresh catalysts to evaluate the aging effects from the various exposures.

3.2.1. FAME-exhaust exposure ($< 0.3\ ppm\ P$ and $2.5\ ppm\ S$ in the fuel)

After aging with pure FAME, mainly the low-temperature (200 – $250^\circ C$) SCR performance of the Cu-SSZ-13 catalysts decreased (Fig. 4, green curves). The NO conversion at $200^\circ C$ decreased from 80 to 64% for the sample aged with a DOC in front (Fig. 4, upper panel to the left). The sample aged with a dummy in front (Fig. 4, lower panel to the left) displayed a somewhat higher degree of deactivation; 59% of the NO

was converted for at $200^\circ C$ this catalyst. A similar effect was seen for the NH_3 conversion for both samples (Fig. 4, middle panels), while the N_2O production (Fig. 4, right panels) decreased from around 16 ppm for the fresh catalyst to around 9 ppm for the aged Cu-SSZ-13. However, at $500^\circ C$, the N_2O production was slightly higher for the aged samples, 8 compared to 6 ppm. The $V_2O_5-WO_3/TiO_2$ catalyst, on the other hand, displayed in principal no deactivation (Fig. 5, green curves). Instead, the sample with a DOC in front during the aging showed a slight promotion in terms of an increase in NO and NH_3 conversion (Fig. 5, upper left and middle panels). Additionally, a decreased N_2O formation was observed for both samples (see Fig. 5, right panels).

3.2.2. Effect of P-doped FAME-exhaust ($93\ ppm\ P$ in the fuel, $2.5\ ppm\ S$)

Exposure to P-doped biodiesel exhaust resulted in a severe deactivation for both the Cu-SSZ-13 and the $V_2O_5-WO_3/TiO_2$ catalyst (orange curves in Figs. 4 and 5, respectively). The Cu-SSZ-13 samples had almost no SCR activity below $300^\circ C$, and even at $500^\circ C$, the conversion does not reach the value of the fresh sample. This is especially pronounced for the sample aged with the dummy in front; at $500^\circ C$, the NO conversion is only 60% for this sample, while it is 82% for the sample with the DOC upstream, compared to 92% for the fresh catalyst. This indicates that the DOC protects the SCR catalysts by capturing part of the phosphorus before it reaches the SCR catalysts. The N_2O production is also totally suppressed at all temperatures for both P-aged Cu-SSZ-13 samples. A severe deactivation

over the entire temperature range is observed also for the $V_2O_5-WO_3/TiO_2$ catalysts, although less severe than for the Cu-SSZ-13 catalyst. Furthermore, the difference between the sample with a DOC core upstream and the sample with a dummy upstream is less pronounced for the $V_2O_5-WO_3/TiO_2$ samples. At $500^\circ C$, the NH_3 conversion is more affected than the NO conversion, indicating that also the unselective ammonia oxidation reactions are inhibited. This is also observed by the suppressed N_2O formation: at $500^\circ C$ the concentration of N_2O decreased from around 55 ppm for the fresh samples (at 10% O_2) to less than 25 ppm for the P-aged samples. The deactivation of the $V_2O_5-WO_3/TiO_2$ over the entire temperature-range due to phosphorus, agrees with that observed in a previous study [10].

3.2.3. Effect of S-doped FAME-exhaust ($130\ ppm\ S$ in the fuel, $0.5\ ppm\ P$)

Sulfur severely inhibits the conversion of NO and NH_3 below $350^\circ C$ for the Cu-SSZ-13 catalyst (Fig. 4, yellow curves, left and middle panels, respectively). The N_2O production at low temperature is also inhibited (Fig. 4, right panels). Similar to the exposure for pure and P-doped FAME exhaust, the deactivation is more pronounced for the sample aged without a DOC core in front. This sample also has a significantly lower NO and NH_3 conversion at 350 and $400^\circ C$; at these temperatures, the sample with the upstream DOC had conversion levels similar to that of fresh catalysts. Another difference between these two Cu-SSZ-13 samples is that at $500^\circ C$, the sample exposed to the S-doped FAME exhaust with a DOC in front displays a slight increase in N_2O formation, compared to fresh catalyst samples. As opposed to this, the sample with the dummy in front during the aging shows a slight decrease in the high-temperature N_2O formation, more similar to the samples exposed to P-doped biodiesel exhaust.

The effect of sulfur on the $V_2O_5-WO_3/TiO_2$ SCR catalyst (Fig. 5, yellow curves) is totally different from that of the Cu-SSZ-13 catalyst. For the sample having a DOC in front during the aging experiment, no deactivation, but rather a promotion is observed for the (Fig. 5, upper panels). This effect is displayed both as an increased conversion of NO and NH_3 , and a decreased high-temperature N_2O selectivity. The N_2O concentration decreased by around 10 ppm, from 55 to 45 ppm. The $V_2O_5-WO_3/TiO_2$ sample aged with an upstream dummy is instead slightly deactivated (Fig. 5, lower panels). This deactivation is seen primarily at $300^\circ C$ and above. Similar to the sample aged with the DOC, the N_2O production at $500^\circ C$ is inhibited; only 35 ppm N_2O was produced for this sample.

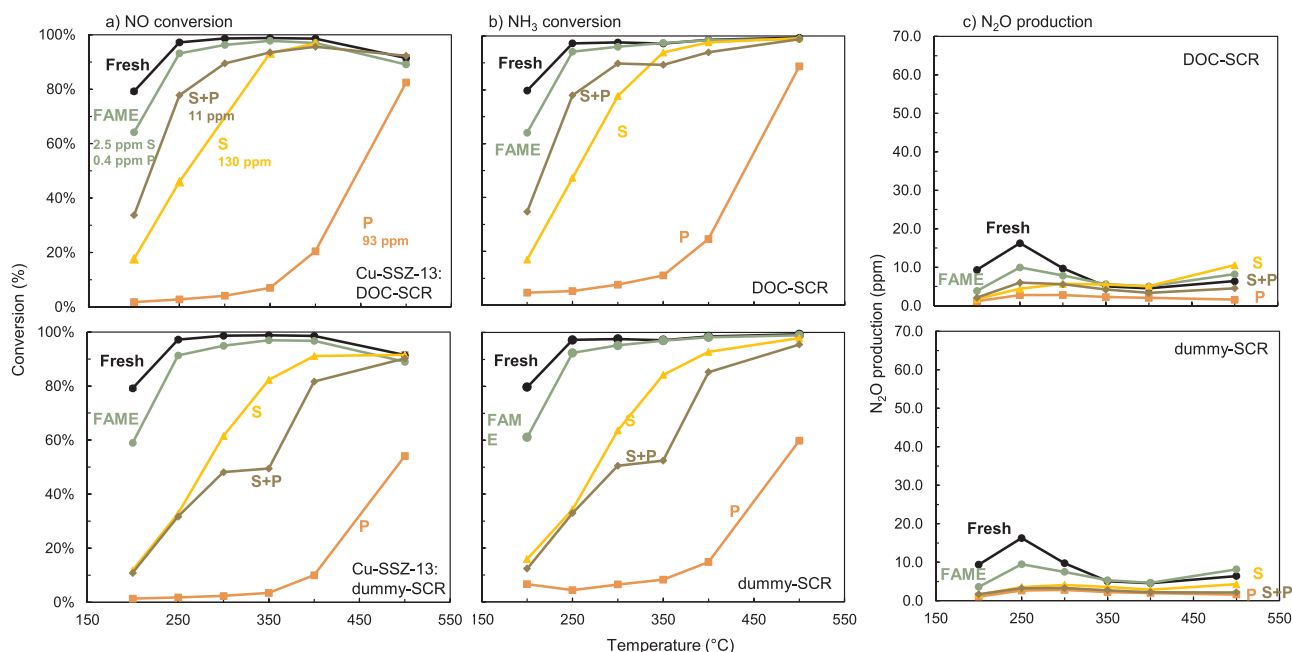


Fig. 4. Effect of exposure to pure (green), P- (orange), S- (yellow), and S + P-doped (brown) biodiesel (FAME) exhaust on NO and NH₃ conversion and N₂O production of Cu-SSZ-13. DOC-SCR or dummy-SCR configuration during aging. Test conditions: 10% O₂, 1000 ppm NO and NH₃, 5% H₂O, GHSV 120,000 h⁻¹.

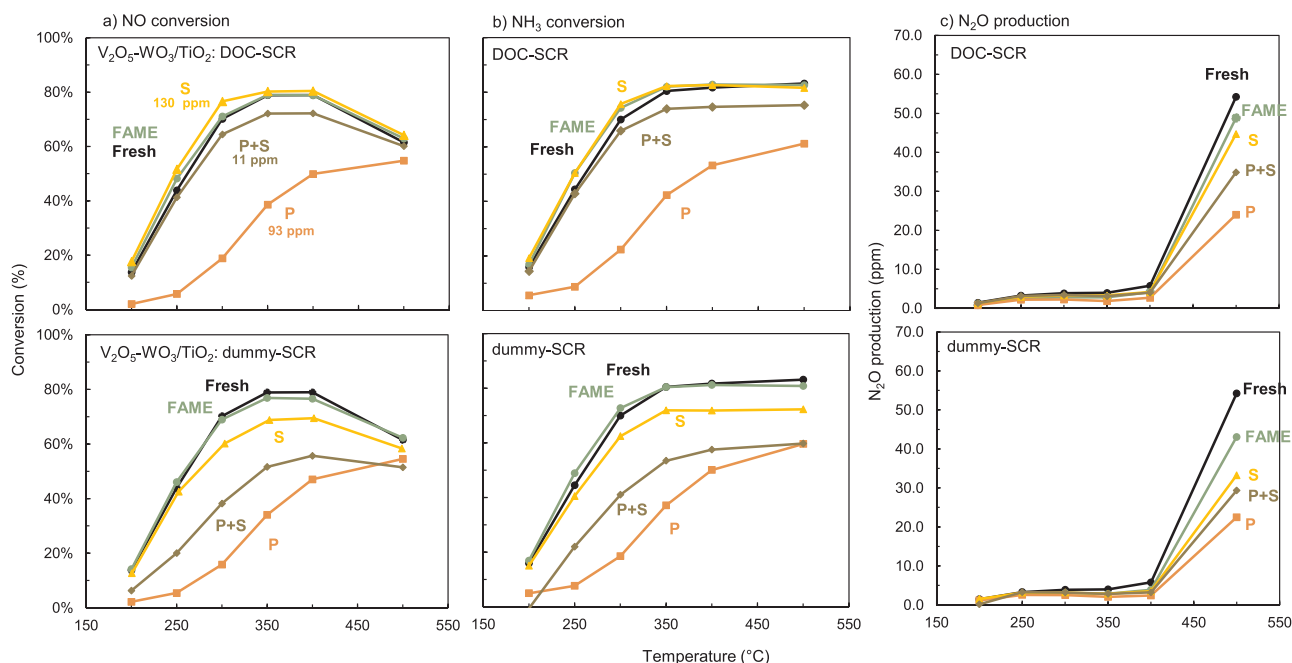


Fig. 5. Effect of exposure to pure (green), P- (orange), S- (yellow), and S + P-doped (brown) FAME exhaust on NO and NH₃ conversion and N₂O production of V₂O₅-WO₃/TiO₂. DOC-SCR or dummy-SCR during aging. Test conditions: 10% O₂, 1000 ppm NO and NH₃, 5% H₂O, GHSV 120,000 h⁻¹.

3.2.4. Effect of P + S-doped FAME exhaust (11 ppm S and P in the fuel)

In the final aging experiment, the biodiesel was doped with both S and P. However, the concentrations of the dopants in the fuel were lower, 11 ppm each of P and S. The most significant effect of this aging with lower contaminant concentrations, is that having an upstream DOC results in a considerably lower degree of deactivation of the SCR catalyst compared to having an upstream dummy. This applies for both the Cu-SSZ-13 and the

V₂O₅-WO₃/TiO₂ catalyst (brown curves in Figs. 4 and 5, respectively). For example, at 200 °C, the NO conversion decreased from almost 80%, for the fresh sample, to 34% for the sample with the DOC in front, and further to only 11% for the sample aged with the dummy.

The corresponding numbers for the V₂O₅-WO₃/TiO₂ samples are 12 and 6%, with upstream DOC and dummy, respectively. At 500 °C, both Cu-SSZ-13 samples reach an NO conversion similar to the fresh samples, while only the V₂O₅-WO₃/TiO₂ sample aged with an upstream DOC reaches a conversion similar to the fresh samples. For the fresh V₂O₅-WO₃/TiO₂ sample and that aged with a DOC in front, the NO conversion at this temperature is around 60%, while only around 50% is reached for the sample that had the dummy in front. The N₂O production decreases for all aged SCR samples, with the largest decrease for those samples that are most severely deactivated. For the Cu-SSZ-13 sample that had the dummy in front, the N₂O production is totally suppressed, similar to the samples exposed to the P-doped FAME-

exhaust. However, the NO and NH₃ conversions are less affected than for the P-aging experiments. Comparing the aging with S + P- with that of S-doped FAME, the samples positioned downstream of a DOC during the aging, displayed a similar effect regarding the formation of N₂O at low temperature. For both these samples, we observed a decreased formation compared to that of fresh catalysts. However, the effect on the high-temperature (500 °C) N₂O formation differs; compared to fresh catalyst, slightly more N₂O is produced for the sample from the S-aging, while instead slightly lower amounts of N₂O is produced after the P + S aging. It thus appears as sulfur inhibits the formation of N₂O at low temperature but might slightly promote it at high temperature, whereas phosphorus appears to inhibit N₂O formation over the entire temperature range. For the V₂O₅-WO₃/TiO₂ catalyst, on the other hand, both phosphorus and sulfur appear to inhibit the high-temperature formation of N₂O.

Summing up the observations for the different exposures, using either a DOC or a dummy upstream of the SCR catalyst, it appears as the DOC traps contaminants, especially phosphorus, making less P available for deactivation of the downstream SCR catalyst sample. This is also confirmed by the elemental analyses of the aged samples, as is shown in section 3.4, and further supported by the significant amounts of phosphorus found in DOCs in previous studies [35,36].

3.3. Sulfur-release from Cu-SSZ-13 during SCR-test – partial regeneration

For most of the Cu-SSZ-13 catalyst samples, we observed a significant amount of SO₂ desorbing during the activity test at 500 °C (See Supplementary information, Fig. S3). Interesting to note is that this desorption started in the test step where ammonia was introduced (no oxygen present), see Fig. S4. At lower temperatures (300–400 °C), or during the temperature ramps, only minor SO₂ desorption was observed.

To investigate the effect of this sulfur removal on the SCR performance, a second SCR test was executed for parts of the aged Cu-SSZ-13 samples after the first test had been done. Expectedly, a partial regeneration of the SCR performance was observed, see Fig. 6. This recovery was observed to be most efficient for the samples that had a DOC in front during the aging, concurrent with the larger amount of SO₂ at 500 °C during the test. The samples that contained phosphorus desorbed a significantly lower amount of SO₂, and consequently the extent of regeneration was lower.

The effect on the SCR performance of having a lower oxygen concentration during the test is also shown in Fig. 6 (right panels). In general, a higher oxygen concentration is favorable for the SCR performance of both aged and partially regenerated, as well as fresh samples. The effect of the SO₂ desorption on the SCR activity with 10% oxygen present in the feed is summarized in Fig. 7, in terms of a relative rate constant. This is defined as the apparent rate constant of the aged catalyst divided by that of the fresh catalyst, $k_{\text{aged}}/k_{\text{fresh}}$ [9]. A significant increase in the relative rate constant at 200–300 °C is observed for most of the samples when comparing the first and the second SCR test results (Fig. 7, full and dotted lines, respectively). However, the P-aged sample showed no, or only a minor recovery, of the low-temperature activity. The same applied for the P + S-aged sample that had a dummy in front during the aging. For the samples exposed to S-doped FAME, the increase in the relative rate constant was significantly higher at 250–300 °C than it was at 200 °C.

N₂O production profiles for the aged and partially regenerated samples can be seen in Fig. S5. The low-temperature N₂O formation increases for most of the partially regenerated samples, but it does not reach the corresponding fresh value except for in the case with the pure FAME-exposed sample with a DOC in front. For this sample, the low-temperature N₂O formation of the regenerated sample is slightly increased compared to the fresh sample. Furthermore, for the partially regenerated sample with the DOC-SCR configuration in the S-doped aging, the N₂O formation is also increased at temperatures between 300

and 500 °C.

3.4. Capture of phosphorus and sulfur in Cu-SSZ-13 and V₂O₅-WO₃/TiO₂ catalysts

After the SCR performance had been tested, elemental analysis was performed on all aged Cu-SSZ-13 and V₂O₅-WO₃/TiO₂ catalyst samples. This analysis showed that both catalysts could capture phosphorus, while only the Cu-SSZ-13 samples captured significant amounts of sulfur (see Tables S2 and S3). No other fuel- or lube-oil related contaminants, such as Na, K, Mg, Ca, or Zn, were detected at any significantly increased levels compared to the fresh material (results not shown). The highest concentration of phosphorus was observed for the V₂O₅-WO₃/TiO₂ catalyst samples exposed to P-doped FAME exhausts (93 ppm P in the fuel); the concentration of P in these samples was around 2 wt%. Note that the uptake of P on these samples is significantly higher than the V content on molar basis: the molar P/V ratios are almost 3. This indicates that the phosphorus in the exhaust interacts not only with the vanadium in this catalyst, but also with other parts of the catalyst material e.g. the WO₃ and/or the TiO₂. Furthermore, no difference is seen between the inlet and the outlet part of these samples. Additionally, SEM-EDX mapping shows that the phosphorus appears to be evenly distributed over the whole substrate, no matter if it is close to the channels where the exhausts enter or in the middle of the substrate wall (see Fig. 8, lower panels).

High concentrations of P were also observed in the Cu-SSZ-13 samples exposed to P-doped FAME exhaust; around 0.3–0.4 wt% P was found in these samples. A phosphorus concentration in the same range as this has previously been observed in the inlet of a Cu-zeolite catalyst that had been aged for 120,000 miles in an engine dynamometer [37]. However, this catalyst there was a strong axial concentration gradient, with a lower concentration in the outlet part of the catalyst [37]. The concentrations of P measured for the samples from the P-doped FAME experiment correspond to molar P/Cu ratios of 1.09 for the sample that had a dummy in front during the aging, and 0.82 for the sample with the DOC in front. The lower concentration of P in the sample with the DOC in front can explain the higher conversion levels reached for this sample, compared to the one aged with the dummy, at temperatures above 350 °C. In both samples, no, or minor, axial gradients were detected. The P/Cu ratio close to 1 at the highest, suggests that as opposed to the V₂O₅-WO₃/TiO₂ catalyst, the phosphorus may interact mainly with the copper in the catalyst. Consequently, P appears to interact more selectively with the copper, than it does with vanadium sites in the V₂O₅-WO₃/TiO₂ catalyst. Based on SEM-EDX mapping, it appears as the phosphorus is rather evenly distributed in the washcoat of the Cu-SSZ-13 catalyst, see Fig. 9, lower panels.

As the concentration of P in the exhaust decreases, the effect of having an upstream DOC became increasingly important. This can be seen when comparing for example the aging experiment with 93 ppm P in the fuel with the experiment with 11 ppm P + 11 ppm S in the fuel. In the latter, there is a considerable difference between the samples with and without an upstream DOC during the aging experiment, both regarding phosphorus concentrations (Tables S2 and S3) and subsequent effect on the SCR performance (Figs. 4 and 5). After the aging with the P + S-doped FAME, the V₂O₅-WO₃/TiO₂ sample with the DOC did not have any elevated levels of P compared to fresh catalyst (i.e. P/V is approximately 0), while the sample with the dummy in front had an average P/V of 1.22. Furthermore, as opposed to the aging with 93 ppm P, an axial phosphorus concentration gradient is observed, with higher concentration of P in the inlet part. For the Cu-SSZ-13 samples, similar results were observed: the average P/Cu was 0.49 for the sample with a dummy in front, while it was less than 0.24 (< 0.1 wt%) for the sample with the DOC in front. As for the V₂O₅-WO₃/TiO₂ sample, there was an axial concentration gradient also in this sample.

Elemental analysis of one of the DOC cores from the aging experiment with the P-doped FAME (93 ppm P in the fuel), showed that high

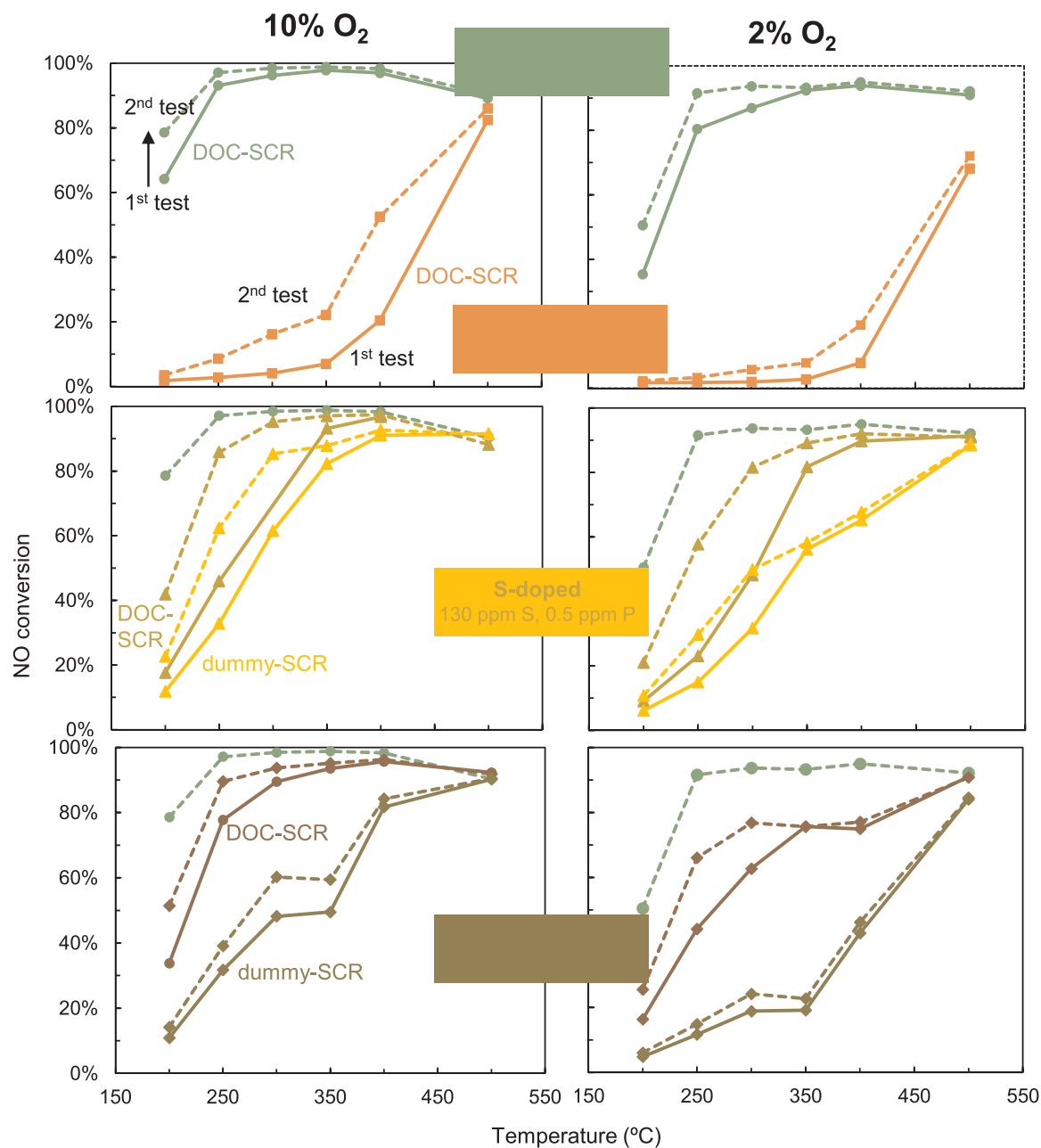


Fig. 6. Effect of SO_2 desorption during the 1st SCR test of the Cu-SSZ-13 cores exposed to pure (green, circles), P- (orange, squares), S- (yellow, triangles), and S + P (brown, diamonds)-doped FAME, as shown by the NO conversion for the 1st test (full lines) and the 2nd test (dotted lines), respectively. The effect of two different oxygen concentrations, 10% (left) and 2% (right), during the SCR tests is shown as well. Test conditions: 2 or 10% O_2 , 1000 ppm NO, 1000 ppm NH_3 , 5% H_2O , GHSV 120,000 h^{-1} .

amounts of phosphorus was present in this sample, around 2.2 wt% (in the whole core i.e. cordierite + washcoat, analyzed by ICP-SFMS). A small concentration gradient was seen between the inlet and the outlet part of this sample, with slightly higher concentrations in the inlet part. The DOC sample from the aging experiment with P + S-doped FAME (11 ppm P, 11 ppm S), had a lower concentration of P, in average 0.85 wt%, and the axial differences in phosphorus concentration were larger. A low concentration of sulfur was observed in this sample, around 0.04 wt%, while no sulfur was detected in the sample from the P-doped aging experiment. The concentration of S on the DOC sample from the S-doped aging experiment was around 0.11 wt%.

Comparing the different aging configurations, i.e. using either a DOC or a dummy in front of the SCR catalyst during the aging experiment, it is concluded that the DOC protects the SCR catalysts from

deactivation by phosphorus through its ability of capturing a large amount of phosphorus. The catalyst samples having a DOC in front during the aging experiments had significantly lower concentrations of phosphorus than the samples aged with a dummy in front.

Based on the concentrations of phosphorus found in the different samples, the concentrations of P in the fuel, and the amount of fuel used, capture efficiencies of P in the different samples were approximated, see Table 4. The assumptions behind these calculated capture efficiencies can be found in the Supplementary Information, Section S5. Higher capture efficiencies are observed for the $\text{V}_2\text{O}_5\text{-WO}_3/\text{TiO}_2$ catalyst than for the Cu-SSZ-13. One explanation for this could be the possibility of P to be captured in the whole core of the $\text{V}_2\text{O}_5\text{-WO}_3/\text{TiO}_2$ sample, as the entire substrate is porous with active material distributed all over it. In contrast to this, the Cu-SSZ-13 sample is washcoated on a

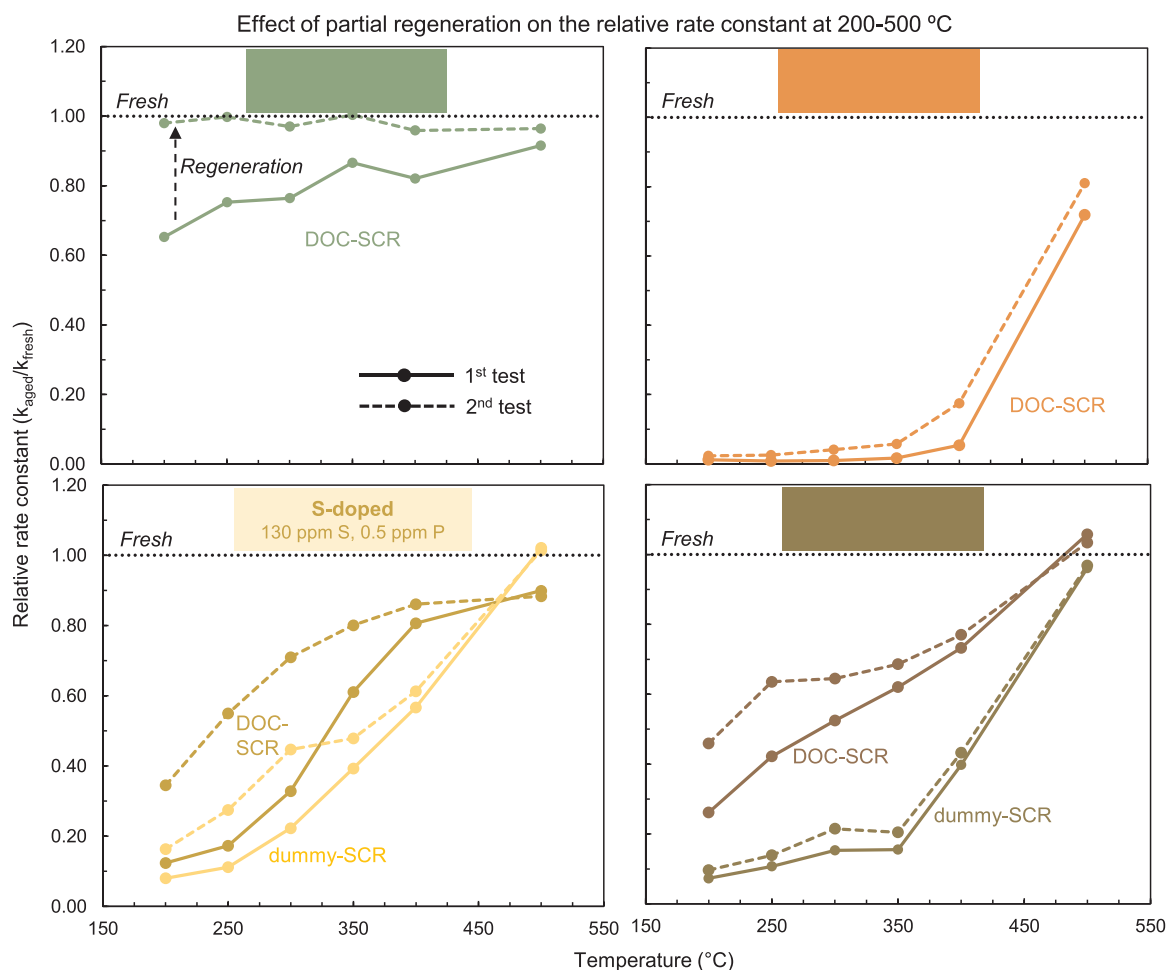


Fig. 7. Effect of SO₂ desorbed during the 1st SCR test on the relative rate constant at 200–500 °C – partial regeneration due to this sulfur removal from the catalyst, as seen when comparing the relative rate constant for the 1st and 2nd SCR tests. Test conditions: 10% O₂, 1000 ppm NO, 1000 ppm NH₃, 5% H₂O, GHSV 120,000 h⁻¹.

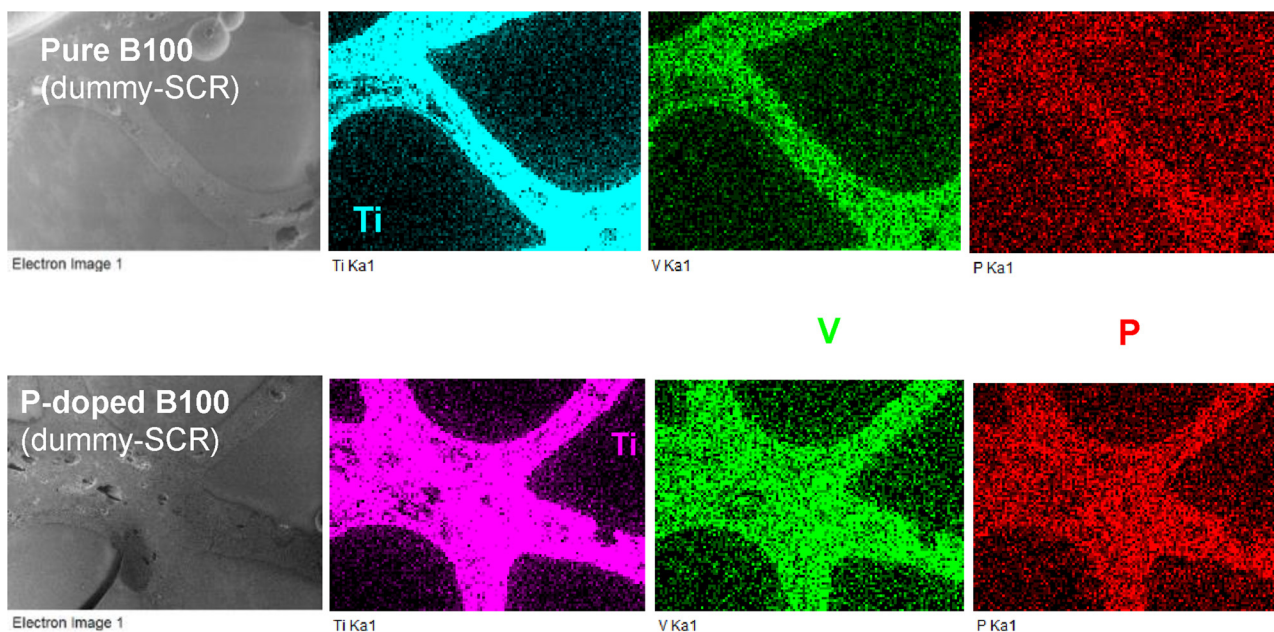


Fig. 8. SEM-EDX mapping of V₂O₅-WO₃/TiO₂ aged with pure FAME (top) and P-doped FAME (bottom) with a dummy upstream during the aging. The sample exposed to P-doped biodiesel exhausts shows high concentration of P all over the catalyst substrate, similar in inlet as in outlet. The sample exposed to pure FAME-exhaust had a slightly increased P-concentration compared to the fresh catalyst, however, based on the mapping it is difficult to distinguish any differences between fresh and FAME-aged sample, as the fresh sample also contains phosphorus. Magnification: 151x.

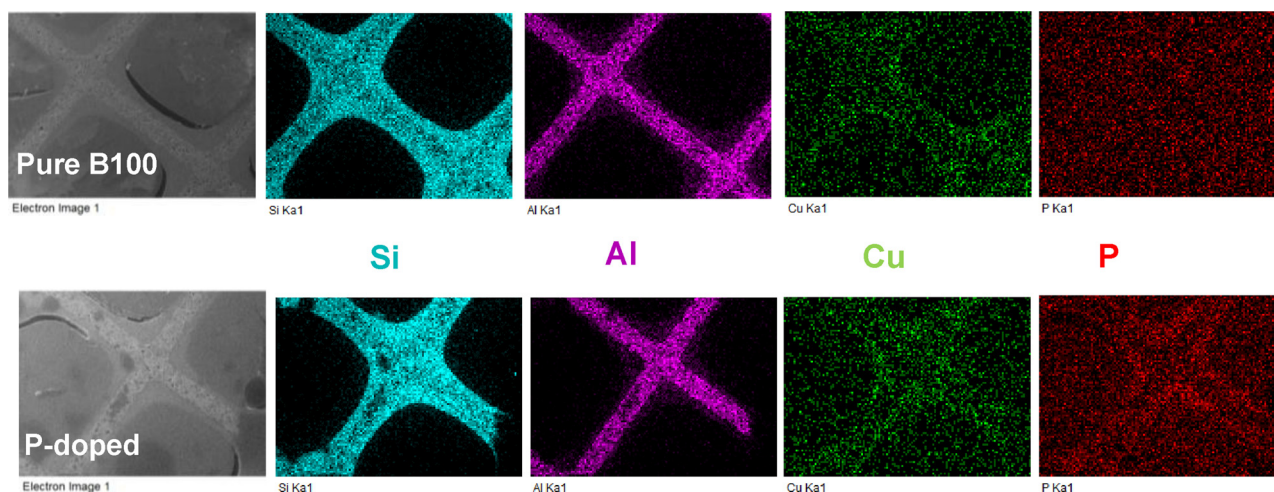


Fig. 9. SEM-EDX mapping of Cu-SSZ-13 samples exposed to pure biodiesel exhaust (top) and P-doped biodiesel exhaust (bottom), with a dummy upstream during the aging. The sample exposed to P-doped FAME exhaust contains P in the whole washcoat thickness, while no P is shown in the mapping for the pure FAME exposed sample. Magnification: 151x.

Table 4

Approximated capture efficiencies of phosphorus in Cu-SSZ-13 and V_2O_5 - WO_3 / TiO_2 . The capture efficiency of a cordierite dummy that had been in the rig for all the aging experiments is displayed as well. Assumptions for the calculated efficiencies are stated in the Supplementary Information, Section S5.

Aging and aging configuration	Capture efficiency of phosphorus (%)	
	Cu-SSZ-13	V_2O_5 - WO_3 / TiO_2
B100, DOC-SCR	na	na
B100, dummy-SCR	na	50 ^a
P-doped B100, DOC-SCR	1	6
P-doped B100, dummy-SCR	1	5
S-doped B100, DOC-SCR	na	na
S-doped B100, dummy-SCR	4 ^a	70 ^a
P + S-doped B100, DOC-SCR	na	6
P + S-doped B100, dummy-SCR	5	18
Dummy (cordierite core), all aging experiments	0.2	

na - not applicable as there was no uptake of P detected within the quantification limits of the performed elemental analysis (< 0.1 wt% P, XRF).

^a Associated with a higher degree of uncertainty, see SI, Section S5.

substrate consisting of less-porous cordierite, and thus the phosphorus can only be captured in a part of the catalysts, i.e. the washcoat.

Furthermore, as stated previously, it appears as phosphorus is deactivating the V_2O_5 - WO_3 / TiO_2 catalyst by fouling the surface non-selectively, while the copper sites in the Cu-zeolite appear to be more selectively poisoned by P.

It is noted that the capture efficiencies for the catalyst samples from the P-doped aging experiments are quite low. This could be due to that the catalysts already have become saturated, or close to saturated, with phosphorus before the aging is finalized. The uniform P concentration throughout the length of both types of SCR catalyst samples, as opposed to the samples from the aging experiment with lower concentration of P in the exhaust, supports this. This is also supported by the previously observed P-gradients on both lab-aged and engine-aged catalysts [7,9,15,17,37]. The almost uniform concentration axially for the DOC samples from this P-doped aging experiment also agrees with this.

For a comparison between the P-uptake of a DOC and a dummy, the capture efficiency of a dummy that had been used during all aging experiments was shown to be very low, around 0.2%.

3.5. SCR performance in relation to contaminant concentration and effect of O_2 concentration in the SCR-test

The various aging experiments and aging configurations, i.e. DOC or dummy upstream of the SCR catalyst, used during these experiments resulted in different amounts of S and P captured in the different SCR catalysts. It is interesting to compare the degree of deactivation with the amount of P and/or S captured by the samples. The low-temperature activity in terms of the relative rate constant at 200 and 250 °C for all aged samples is correlated to the total contamination level in these samples (see Figs. 10 and 11). For the Cu-SSZ-13 samples, the x-axis consists of the sum of the molar P/Cu and S/Cu ratios, as both P and S were captured in these samples. For the V_2O_5 - WO_3 / TiO_2 samples, the molar P/V ratio is on the x-axis. In these figures, the result of using two different oxygen concentrations (10% O_2 - black circles, and 2% O_2 - blue squares) during the SCR test is displayed as well. For the Cu-SSZ samples, both aged (full symbols) and partially regenerated (empty symbols) samples are included. The partially regenerated data originates from the second SCR test performed for the majority of the Cu-SSZ-13 catalysts after the first test of the SCR performance. From Fig. 10 it can be concluded that a rather low contamination level results in a quite high degree of deactivation for the Cu-SSZ-13 catalyst. Table S5 provides a list with the P/Cu + S/Cu values of aged and partially regenerated samples for the different aging experiments and configurations.

Comparing the deactivating effect of sulfur with that of phosphorus, we noted that rather similar molar ratios of S or P per Cu result in quite different degrees of deactivation: a S/Cu ratio of 0.75 leads to a relative rate constant of 0.13 and 0.18 at 200 and 250 °C, respectively, while the corresponding values for the sample with a P/Cu of 0.82 results in a relative rate constant of only 0.01 at both temperatures. Furthermore, the P-poisoned sample (P/Cu = 0.82) shows considerably lower NO conversion also at higher temperatures, 300–400 °C, than does the S-poisoned sample (S/Cu = 0.75), see Table 5.

Another interesting observation is that for some of the aged samples, the dependence of the oxygen concentration in the test feed appears to be stronger than for others. For these samples, a higher oxygen concentration results in a significantly higher relative rate constant, and this dependence appears to be stronger at 250 °C compared to 200 °C.

The V_2O_5 - WO_3 / TiO_2 samples show less deactivation at low temperature than the Cu-SSZ-13, even for higher contamination levels (note the different scales on the x-axis for the different catalysts: P/V = 0–3.5 compared to the (P/Cu + S/Cu) = 0–1.5). Interestingly, at 200 °C, a lower oxygen concentration appears to be favorable for the

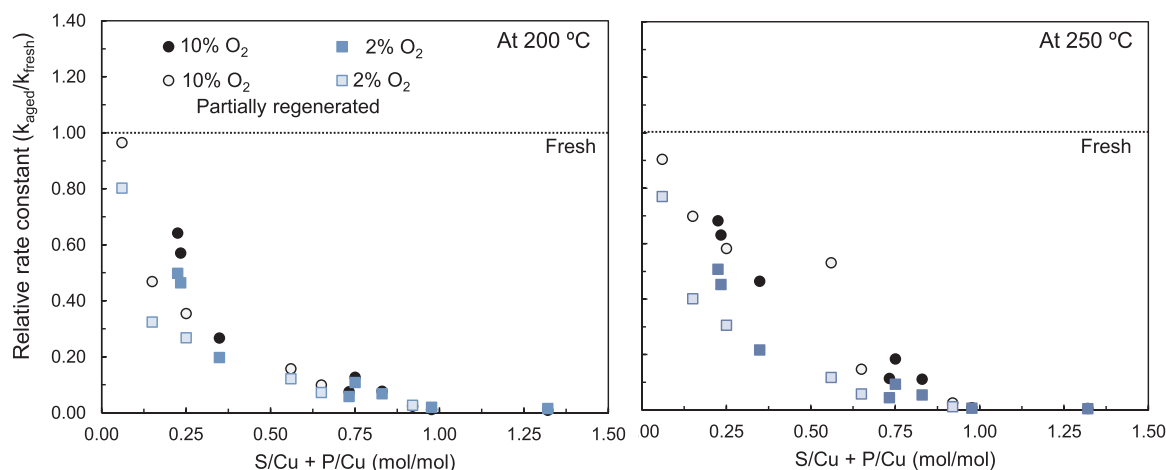


Fig. 10. Relative rate constant of as-received (1st SCR test, full circles) and partially regenerated (2nd SCR test, empty circles) Cu-SSZ-13 samples at 200 (left) and 250 °C (right), as function of molar S/Cu + P/Cu, and for two different O₂ concentrations (2 and 10%). The amount of S is based on both the elemental analysis performed after the SCR tests, and on the estimated amount of SO₂ desorbed during the 500 °C-performance test. Inlet concentrations during SCR test: 2 or 10% O₂, 1000 ppm NO, 1000 ppm NH₃, 5% H₂O; GHSV: 120,000 h⁻¹.

samples containing high amounts of phosphorus, while at 250 °C no, or only a minor, effect of O₂ concentration is observed. Also worth noting though, is that while the *low-temperature* performance of the vanadium-based catalyst samples was less severely affected by the agings than was the performance for the Cu-zeolite samples, the *high-temperature* performance of the vanadium-based catalyst was generally more affected. This again, could be an indication of a more non-selective chemical deactivation for the V₂O₅-WO₃/TiO₂ catalyst, whereas a more selective poisoning appears to occur for the Cu-SSZ-13 catalyst.

4. Conclusions

In this work, the durability of Cu-SSZ-13 and V₂O₅-WO₃/TiO₂ SCR catalysts towards sulfur and phosphorus exposure was investigated. This was performed by aging the catalysts with exhausts of either pure, P-, S-, or P + S-doped biodiesel. SCR performance tests of fresh and exposed catalyst samples were conducted, as well as elemental analyses of the aged catalyst samples after performing the SCR tests. Based on this, we can conclude the following:

- Both the Cu-SSZ-13 and the V₂O₅-WO₃/TiO₂ catalysts capture phosphorus. The V₂O₅-WO₃/TiO₂ catalyst captures a larger amount

of phosphorus, molar P/V ratios above 2.5 are observed for this catalyst, while the molar P/Cu ratio is at the highest slightly above 1 for the Cu-SSZ-13.

- Phosphorus exposure results in severe deactivation of both types of SCR catalysts over the entire temperature range 200–500 °C. However, the Cu-SSZ-13 catalyst is more severely deactivated by phosphorus than the V₂O₅-WO₃/TiO₂ catalyst, especially at low-intermediate temperatures.
- The two points above combined suggest that phosphorus is not only related to vanadium in the V₂O₅-WO₃/TiO₂ catalyst while it appears to poison copper in the Cu-SSZ-13 catalyst more selectively.
- In all aging experiments, the SCR catalysts aged with an upstream dummy, displayed more severe deactivation than the samples that had an upstream DOC. Thus, an upstream DOC protects a downstream SCR catalyst by capturing phosphorus, causing lower amounts of phosphorus to reach the SCR catalyst.
- Cu-SSZ-13 captures sulfur while the V₂O₅-WO₃/TiO₂ catalyst does not, or only minor amounts. Exposure to sulfur results in severe deactivation of the low-temperature performance of the Cu-SSZ-13 catalyst while the V₂O₅-WO₃/TiO₂ catalyst instead is slightly promoted by sulfur.
- Partial removal of sulfur from the Cu-SSZ-13, with subsequent

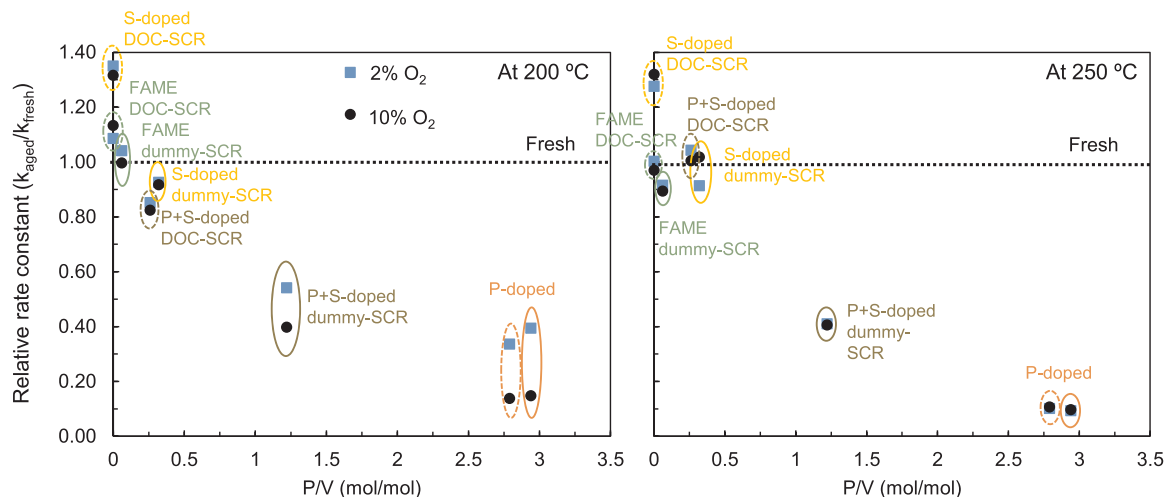


Fig. 11. Relative rate constant of V₂O₅-WO₃/TiO₂ at 200 (left) and 250 °C (right), as function of molar P/V ratio for two different O₂ concentrations, 2 and 10%. Inlet concentrations during SCR test: 2 or 10% O₂, 1000 ppm NO, 1000 ppm NH₃, 5% H₂O; GHSV: 120,000 h⁻¹.

Table 5

Comparison of the performance at high and low temperatures of catalyst samples that contain either mainly sulfur or mainly phosphorus.

	Mainly S-poisoned Cu-SSZ-13 sample ¹	Mainly P-poisoned Cu-SSZ-13 sample ²	P-poisoned V ₂ O ₅ -WO ₃ /TiO ₂ ³
P/Cu or V	0.01 ^a	0.82	1.22
S/Cu or V	0.75	0.16	0.00
k _{aged} /k _{fresh} at 200 °C	0.13	0.01	0.40
k _{aged} /k _{fresh} at 250 °C	0.18	0.01	0.37
NO conversion at 300 °C (fresh)	0.76 (0.98)	0.04 (0.99)	0.38 (0.71)
NO conversion at 400 °C (fresh)	0.97 (0.98)	0.21 (0.99)	0.55 (0.79)
NO conversion at 500 °C (fresh)	0.89 (0.90)	0.83 (0.92)	0.52 (0.64)

¹ S-doped FAME, DOC-SCR sample.² P-doped FAME, DOC-SCR sample.³ P + S-doped FAME, dummy-SCR.^a Based on quantification by SEM-EDX. < 0.1 wt% according to the XRF analysis.

partial recovery of the SCR performance, occurs during the SCR test at 500 °C. Especially, the SO₂ desorption seems to be promoted by the NH₃ introduction. Furthermore, less SO₂ desorption and only minor regeneration is observed for Cu-SSZ-13 samples that contain phosphorus (P > 0.1 wt%).

- The aging with pure FAME resulted in a decreased low-temperature performance of Cu-SSZ-13. This decrease was at least partially due to sulfur, as an improved SCR performance was observed after SO₂ had desorbed during the first SCR test. The V₂O₅-WO₃/TiO₂ catalyst instead showed a slightly improved SCR performance by the FAME exposure.

This study provides useful information in choosing appropriate types of catalysts and exhaust system configurations for various applications. In addition, insights from this work could aid the development of more durable catalysts.

CRedit authorship contribution statement

Sandra Dahlin: Conceptualization, Methodology, Validation, Formal analysis, Investigation, Data curation, Writing - original draft, Writing - review & editing, Visualization. **Johanna Englund:** Conceptualization, Methodology, Investigation, Writing - review & editing. **Henrik Malm:** Investigation, Resources. **Matthias Feigel:** Software, Formal analysis. **Björn Westerberg:** Methodology, Software, Resources. **Francesco Regali:** Conceptualization. **Magnus Skoglundh:** Conceptualization, Writing - review & editing, Supervision. **Lars J. Pettersson:** Conceptualization, Writing - review & editing, Supervision.

Declaration of Competing Interest

There are no conflicts to declare.

Acknowledgements

The Swedish Energy Agency, as well as the collaboration partners Scania CV AB, Umicore Denmark ApS, and Volvo Group Trucks Technology, are gratefully acknowledged for the financial support of this FFI project (FFI project No 37178-1). An additional thanks to Ton V.W. Janssens and Peter S. Hammershøi at Umicore Denmark ApS for arranging with the elemental analyses (Leco, ICP, XRF) of the catalyst samples and the biodiesel.

Appendix A. Supplementary data

Supplementary material related to this article can be found, in the online version, at doi:<https://doi.org/10.1016/j.cattod.2020.02.018>.

References

- [1] J. Granstrand, S. Dahlin, O. Immele, L. Schmalhorst, C. Lantto, M. Nilsson, R.S. Paris, F. Regali, L.J. Pettersson, *RSC Catalysis* 30 (2018) 64.
- [2] Neste Oil Oyj, Hydrotreated vegetable oil (HVO) - premium renewable biofuel for diesel engines, Espoo, March, 2014.
- [3] F. Gao, C. Peden, *Catalysts* 8 (2018) 140.
- [4] J. Jansson, Vanadia-Based Catalysts for Mobile SCR, in: I. Nova, E. Tronconi (Eds.), Urea-SCR technology for deNOx after treatment of diesel exhaust, Springer, New York, 2014, pp. 65–96.
- [5] I. Lezcano-Gonzalez, U. Deka, H.E. van der Bij, P. Paalanen, B. Arstad, B.M. Weckhuysen, A.M. Beale, *Appl. Catal. B* 154–155 (2014) 339.
- [6] K. Xie, K. Leistner, K. Wijayanti, A. Kumar, K. Kamasamudram, L. Olsson, *Catal. Today* 297 (2017) 46.
- [7] K. Xie, A. Wang, J. Woo, A. Kumar, K. Kamasamudram, L. Olsson, *Appl. Catal. B* 256 (2019) 117815.
- [8] Z. Chen, C. Fan, L. Pang, S. Ming, P. Liu, T. Li, *Appl. Catal. B* 237 (2018) 116.
- [9] S. Dahlin, C. Lantto, J. Englund, B. Westerberg, F. Regali, M. Skoglundh, L.J. Pettersson, *Catal. Today* 320 (2019) 72.
- [10] H. Kamata, K. Takahashi, C.U.I. Odenbrand, *Catal. Lett.* 53 (1998) 65.
- [11] M. Klimczak, P. Kern, T. Heinzelmann, M. Lucas, P. Claus, *Appl. Catal. B* 95 (2010) 39.
- [12] O. Kröcher, M. Elsener, *Appl. Catal. B* 77 (2008) 215.
- [13] D. Nicosia, M. Elsener, O. Kröcher, P. Jansohn, *Top. Catal.* 42–43 (2007) 333.
- [14] F. Castellino, S.B. Rasmussen, A.D. Jensen, J.E. Johnsson, R. Fehrmann, *Appl. Catal. B* 83 (2008) 110.
- [15] R. Eschrich, J. Schröder, F. Hartmann, R. Gläser, *MTZ worldwide* 76 (2014) 44.
- [16] J. Blanco, P. Avila, C. Barthelemy, A. Bahamonde, J.A. Odriozola, J.F.G. De La Banda, H. Heinemann, *Appl. Catal.* 55 (1989) 151.
- [17] J. Englund, Deactivation of SCR catalysts - Impact of sulfur and the use of biofuels, Lic. Eng. Thesis Department of Chemistry and Chemical Engineering, Division of Applied Surface Chemistry, Competence Centre of Catalysis, Chalmers University of Technology, Gothenburg, Sweden, 2018.
- [18] S. Dahlin, J. Englund, F. Regali, M. Skoglundh, L.J. Pettersson, Investigation of fuel and lube oil contaminants on Cu-SSZ-13 and V₂O₅-WO₃/TiO₂ SCR catalysts, CEC&EECAT, Tianjin, China, (2018).
- [19] P.S. Hammershøi, A.D. Jensen, T.V.W. Janssens, *Appl. Catal. B* 238 (2018) 104.
- [20] P.S. Hammershøi, Y. Jangjou, W.S. Epling, A.D. Jensen, T.V.W. Janssens, *Appl. Catal. B* 226 (2018) 38.
- [21] P.S. Hammershøi, A.L. Godiksen, S. Mossin, P.N.R. Vennestrøm, A.D. Jensen, T.V.W. Janssens, *React. Chem. Eng.* 4 (2019) 1081.
- [22] Y. Wang, Z. Li, R. Fan, X. Guo, C. Zhang, Y. Wang, Z. Ding, R. Wang, W. Liu, *Catalysts* 9 (2019) 797.
- [23] K. Wijayanti, K. Leistner, S. Chand, A. Kumar, K. Kamasamudram, N.W. Currier, A. Yezerets, L. Olsson, *Catal. Sci. Technol.* 6 (2016) 2565.
- [24] J. Luo, D. Wang, A. Kumar, J. Li, K. Kamasamudram, N. Currier, A. Yezerets, *Catal. Today* 267 (2016) 3.
- [25] R. Ando, T. Hihara, Y. Banno, M. Nagata, T. Ishitsuka, N. Matsubayashi, T. Tomie, Detailed Mechanism of S Poisoning and De-Sulfation Treatment of Cu-SCR Catalyst, *SAE International* (2017).
- [26] W. Su, Z. Li, Y. Zhang, C. Meng, J. Li, *Catal. Sci. Technol.* 7 (2017) 1523.
- [27] A. Kumar, M.A. Smith, K. Kamasamudram, N.W. Currier, H. An, A. Yezerets, *Catal. Today* 231 (2014) 75.
- [28] Y. Cheng, C. Lambert, D.H. Kim, J.H. Kwak, S.J. Cho, C.H.F. Peden, *Catal. Today* 151 (2010) 266.
- [29] S.L. Bergman, S. Dahlin, V.V. Mesilov, Y. Xiao, J. Englund, S. Xi, C. Tang, M. Skoglundh, L.J. Pettersson, S.L. Bernasek, In-situ studies of oxidation/reduction of copper in Cu-CHA SCR catalysts: comparison of fresh and SO₂-poisoned catalysts, *Appl. Catal. B* (2019) Submitted manuscript.
- [30] A.R. Fahami, T. Günter, D.E. Doronkin, M. Casapu, D. Zengel, T.H. Vuong, M. Simon, F. Breher, A.V. Kucherov, A. Brückner, J.D. Grunwaldt, *React. Chem. Eng.* 4 (2019) 1000.
- [31] T.J. Toops, J.A. Pihl, W.P. Partridge, Fe-Zeolite Functionality, Durability, and Deactivation Mechanisms in the Selective Catalytic Reduction (SCR) of NOx with

- Ammonia, in: I. Nova, E. Tronconi (Eds.), Urea-SCR technology for deNO_x after treatment of diesel exhaust, Springer, New York, 2014, pp. 97–121.
- [32] C. Ciardelli, I. Nova, E. Tronconi, D. Chatterjee, B. Bandl-Konrad, M. Weibel, B. Krutzsch, *Appl. Catal. B* 70 (2007) 80.
- [33] K. Leistner, O. Mihai, K. Wijayanti, A. Kumar, K. Kamasamudram, N.W. Currier, A. Yezerets, L. Olsson, *Catal. Today* 258 (2015) 49.
- [34] T.V. Johnson, Review of Selective Catalytic Reduction (SCR) and Related Technologies for Mobile Applications, in: I. Nova, E. Tronconi (Eds.), Urea-SCR technology for deNO_x after treatment of diesel exhaust, Springer, New York, 2014, pp. 3–31.
- [35] A. Winkler, D. Ferri, M. Aguirre, *Appl. Catal. B* 93 (2009) 177.
- [36] J. Granstrand, R.S. Paris, U. Nylén, M. Nilsson, L.J. Pettersson, Effects of soot, sulphur, sodium, calcium and phosphorus on diesel oxidation catalyst after operation in a FAME biodiesel-fueled heavy-duty vehicle, 18th Nordic Symposium on Catalysis, Copenhagen, Denmark, August, 2018.
- [37] Y. Cheng, L. Xu, J. Hangan, M. Jagner, C. Lambert, Laboratory Postmortem Analysis of 120k mi engine aged urea SCR catalyst, SAE International (2007).